Computation of a Highly Saturated Permanent Magnet Synchronous Motor for a Hybrid Electric Vehicle

Stefan Henneberger, Uwe Pahner, Kay Hameyer and Ronnie Belmans
Katholieke Universiteit Leuven, E.E. Dept., Div. ESAT/ELEN
Kardinaal Mercierlaan 94, B-3001 Leuven, Belgium

***Abstract* - In the framework of the development of a drive system for the implementation in a hybrid electric vehicle, a 45 kW 6-pole permanent magnet synchronous motor (PMSM) is designed. Due to the rotor design with inset permanent magnets the machine parameters are dependant on the operating point due to saturation effects. Numerical computations using the finite element method (FEM) are performed to build up a lumped parameter model of the machine.**

I. Introduction

Inset NdFeB permanent magnets, a high current density and special control strategies are applied in order to achieve requirements such as extended field weakening range and high power/weight ratio. One of the main design goals for the studied drive system is the continuous operation of the PMSM at high efficiency. Therefore, a rotor geometry with $X_q > X_d$ is chosen to benefit from an additional reluctance torque (Fig.1) [1],[2]. The rotor design causes a disadvantage for the motor control: The machine parameters are dependant on the operating point due to saturation effects. As a real time control strategy is essential to assure the continuous operation at highest efficiency, those dependencies have to be known beforehand. The control algorithm then directly operates on the pre-calculated set of performance characteristics in form of tables or polynomial functions.

II. Advanced Field Weakening

The motor operates in an advanced field weakening mode by implementing a negative direct stator current in order to benefit from the reluctance torque. The motor can be operated in two modes. In the constant torque mode, the speed of the drive is increased by raising the stator frequency and voltage until rated speed is reached. To increase speed further, power and voltage have to be maintained constant while increasing the angle between stator current and field axis above 90º by additionally applying a negative direct stator current component (Fig. 2). The required current is minimized and the possibility of irreversibly demagnetizing the magnets is reduced. The significant saliency of the motor, realized by constructing a rotor with surface-inset magnets (Fig. 1), is generating a reluctance torque.

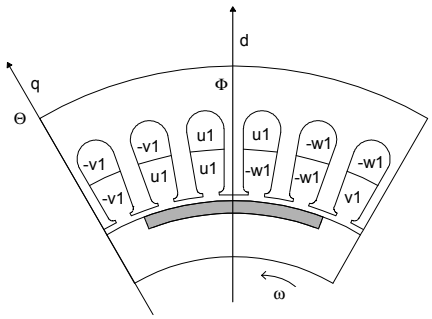

Fig. 1. Cross-sectional view of a 6-pole surface-inset PMSM.

The torque equation is a function of the angle $\Psi = 90º-\delta$ and can be splitted into an electromagnetic component (1) and a reluctance component (2)

$$T_e(\Psi) = \frac{m \cdot p}{\omega_0} \cdot E \cdot I_q \ , \tag{1}$$

$$T_r(\Psi) = m \cdot p \cdot I_d \cdot I_q \cdot \left(L_q - L_d\right), \tag{2}$$

where $I_d = I \cdot \sin(\Psi)$, $I_q = I \cdot \cos(\Psi)$ with m - the number of phases, p - the number of poles, ω_0 - the synchronous angular speed and E - the fundamental e.m.f..

The motor is controlled by adjusting the load angle to obtain the maximum torque $T_{max} = T_e + T_r$ which is expressed as a function of the angle $\Psi = 90º-\delta$ by the equation

$$\Psi_{opt} = \arcsin\left(\frac{E}{4 I_1 \omega \left(L_q - L_d\right)} - \sqrt{\left(\frac{E}{4 I_1 \omega \left(L_q - L_d\right)} \right)^2 + \frac{1}{2}} \right). \tag{3}$$

Using ideal constant values of the inductance obtained by

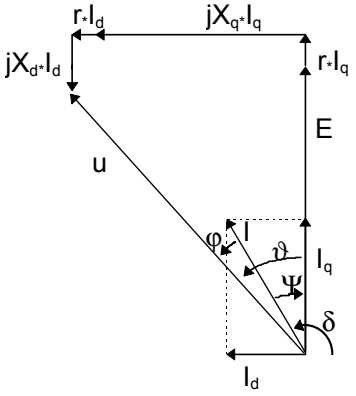

Fig. 2. Phasor diagram of the PMSM in the advanced field weakening mode.

Manuscript received January 31, 1997.
Stefan Henneberger, stefan.henneberger@esat.kuleuven.ac.be; Uwe Pahner, uwe.pahner@esat.kuleuven.ac.be; Kay Hameyer, kay.hameyer@esat.kuleuven.ac.be; Ronnie Belmans, ronnie.belmans@esat.kuleuven.ac.be;
Co-ordinates for all authors: Tel.: +32-16-32.10.20, Fax.: +32-16-32.19.85;
Internet: http://www.esat.kuleuven.ac.be/elen/elen.html.

analytical calculation as well as by linear numerical computation, equation (3) yields an optimum load angle of Ψ_{opt}=22º at the rated current I_r. However, the numerically computed torque using a non-linear model has a maximum value at Ψ=39º (Fig. 3). Furthermore, the maximum value of the numerical computed torque is about 10% higher as the analytically predicted result. In the linear analysis, the reluctance torque characteristics have a symmetry at the maximum angle Ψ=45º. A non-linear analysis shows a shift of the maximum value to an angle Ψ=50º when the current is increased. Due to saturation effects in the stator teeth and the rotor iron in the pole gap, the inductances L_d and L_q are the function of the stator current and the load angle or, in other words of the current components I_d and I_q. They have to be known for each possible state of operation in order to control the machine as well as to simulate the dynamic behaviour of the machine.

III. Two-Dimensional Finite Element analysis

The application of the finite element analysis for the determination of the lumped parameter model and the performance of the PMSM have been discussed widely in the literature [5],[6]. As shown in [5], the FE analysis is suited for the calculation of the PMSM utilizing rotor geometry with $X_q > X_d$.

As the real time control scheme requires a whole set of performance characteristics, a high number of FE model evaluations has to be performed. A static non-linear problem definition is applied. The torque of the motor can be

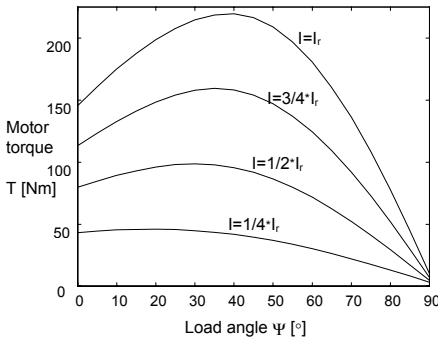

Fig. 3. Numerical computed overall torque as function of the load angle at different stator currents.

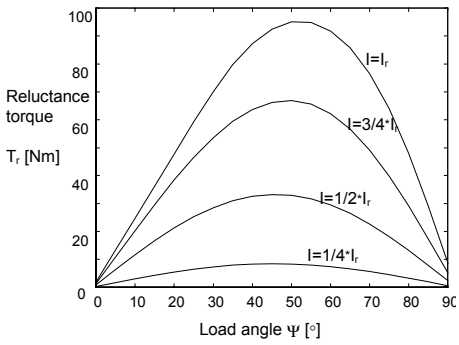

Fig. 4. Numerical computed reluctance torque as function of the load angle at different stator currents.

determined using the virtual work method or the Maxwell stress tensor method. The application of the virtual work method requires two FE computations per operation point, which disqualifies this method for such a high number of evaluations. The classical Maxwell stress tensor method, however, is known to be very unreliable, as it is based on numerical derivatives of the potential solution. A newly developed method has been applied for the torque computation, which is based on a local solution of Laplace's equation in a post-process [7]. In this method, the numerical derivatives for the components of the flux density are replaced by derivatives of a Fourier series. This Fourier series (4) represents the solution of the Laplace equation in a circular 2D domain. The known potentials A_{zi} (from the FE solution), at N equi-angular ordered points on the circumference of the circle with radius R, (Fig.5) are the boundary values to determine the Fourier coefficients of order k (5).

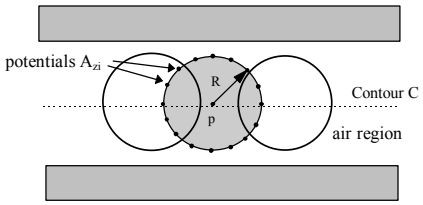

Fig. 5. Considered domain for the Laplace solution inside the machine air gap

$$A_z(r,\vartheta) = \frac{a_0}{2} + \sum_{k=1}^{M}\left(a_k r^k \cos(k\vartheta) + b_k r^k \sin(k\vartheta) + c_k r^{-k}\cos(k\vartheta) + d_k r^{-k}\sin(k\vartheta)\right) \tag{4}$$

$$a_k = \frac{2}{N\cdot R^k}\sum_{i=1}^{N} A_i \cos(k\vartheta_i) \tag{5}$$

$$b_k = \frac{2}{N\cdot R^k}\sum_{i=1}^{N} A_i \sin(k\vartheta_i)$$

Using (4), the components of the flux density can now be derived analytically (6, 7).

$$B_x = \left.\frac{\partial A_z(x,y)}{\partial y}\right|_p = b_1 \tag{6}$$

$$B_y = -\left.\frac{\partial A_z(x,y)}{\partial x}\right|_p = -a_1 \tag{7}$$

By deriving analytically, the convergence order of the error of the local field quantities remains the same as for the potential solution itself. This procedure is repeated along the integration contour C inside overlapping domains.

Substituting the numerically derived components of the flux density in the Maxwell stress tensor with the components found by (6, 7) leads to a high accuracy of the computed

torque. The convergence of the error of this method has been investigated in [7],[8]. The calculation of the inductances L_d and L_q as a function of the load angle δ_1 is straightforward, applying a flux linkage method. Formulation (8) [4] provides the general tool to compute the inductance of a winding in two dimensions,

$$L = \frac{l_z}{i^2}\int_S A_z \cdot J\, dS \tag{8}$$

where:

A_z - the vector potential,
l_z - the stack length of the stator,
S - the surface of the cross section of the slots that carry the current of the appropriate winding,
i - the current per strand,
J - the current density.

The number of windings is considered by the dependency of the current density J from the current per strand i. One non-linear model is solved for each studied load angle. In the post-process, the appropriate distributions of J, conforming to I_d or I_q, are generated. L_d and L_q are extracted using (8). Due to the non-linear problem definition, the saturation dependencies of the inductances are found.

To cover the whole operation range of the motor, the inductances L_d and L_q are computed for in the step of $\Delta\delta$=5º and ΔI=0.05*I_r. This involves 380 FE solutions. The results for I=I_r are indicated in Fig. 5. The graph shows the difference $\Delta L = L_q$-L_d for two selected load angles δ_a and δ_b. ΔL rises if δ increases, due to the saturation of the d-axis flux path.

This predicts the variation of the inductances $L_q(I,\delta)$ and $L_d(I,\delta)$ can be used in the control algorithm. Equation (3) becomes a differential equation $\Psi_{opt}(I,\Psi)$ and can be solved by using tables of the numerical computed values (Fig. 6,7). For real time control algorithms the inductances are approximated by polynomial functions.

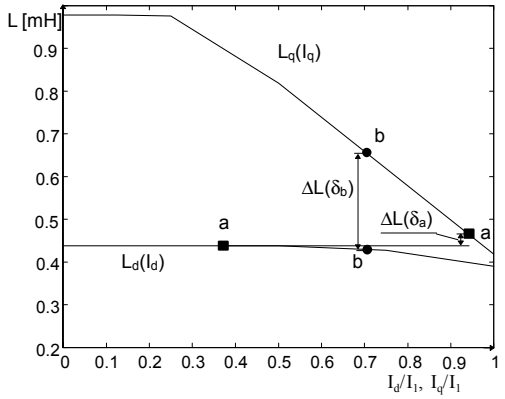

Fig. 6. Inductances L_d and L_q as function of the current components I_d and I_q for two different load angles at rated current.

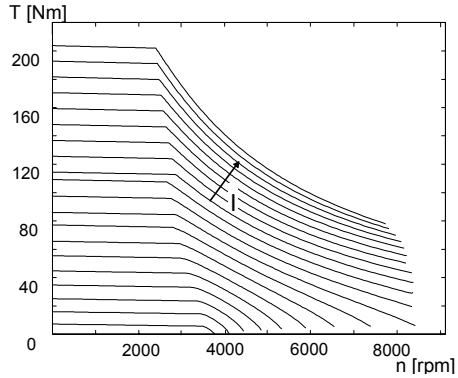

Fig. 7. Torque as function of the speed obtained by static calculation of the equivalent circuit using $L_q(I,\delta)$ and $L_d(I,\delta)$.

IV. Conclusion

In this paper, the calculation of the performance characteristics of a highly saturated 45 kW 6-pole PMSM has been given. The accurate prediction of the motor performance is essential for the optimal control of the drive over a wide range of operation. The influence of the saturation effects on the motor torque is considered. The inductances L_d and L_q are computed for each operational point as a basis for the implementation of a real time control scheme to operate the motor in field weakening mode.

Acknowledgement

The authors are grateful to the Belgium Ministry of Scientific Research for granting the IUAP No. P4/20 on Coupled Problems in Electromagnetic Systems and the Council of the Belgian National Science Foundation.

References

[1] S. A. Nasar , I. Boldea , L. E. Unnewehr , *Permanent Magnet, Reluctance, and Self-Synchronous Motors*. CRC Press, 1993, London Tokyo

[2] St. Henneberger , St. Van Haute, K. Hameyer, R. Belmans, "Design of a 45 kW Permanent Magnet Synchronous Motor for a Hybrid Electric Vehicle", *IMACS*, St. Nazaire, Sept. 17-19, 1996, Conf. Proc. Vol.1, pp. 151-156

[3] J.-M. Kim, S.-K. Sul, "Speed Control of Permanent Magnet Synchronous Motor Drive for Flux Weakening Operations", *IAS'95*, 1995, Conf. Proc., pp. 216-211.

[4] D.A. Lowther, P.P. Silvester, *Computer Aided Design in Magnetics*, Springer Verlag, Berlin , Heidelberg, New York, Tokyo, 1986

[5] G. Henneberger, S. Domack and J. Berndt, "Comparison of the Utilization of Brushless DC Servomotors with Different Rotor Length y 3D - Finite Element Analysis", *IEEE Transactions on Magnetics*, vol. 30, no. 5, pp. 3675-3678, 1994

[6] D. Taghezout and P. Lombard, "Finite Element Prediction of a Brushless DC Motor Dynamical Behaviour", *2nd EPE Chapter Symposium on Electric Drive Design and Applications*, Nancy, France, June 4-6, 1996, Conf. Proc. pp. 47-52

[7] U.Pahner, R.Mertens, K.Hameyer, R.Belmans: "Comparison of two post-processing techniques in 2D FEM based on local solutions of the Laplace equation" *ICEM 1996*, Vigo, Spain, 10-12 Sept. 1996, Conf. Proc. Vol.1, pp.131-136.

[8] R.Mertens, U.Pahner, K.Hameyer, R.Belmans, R.De Weerdt: "Force calculation based on a local solution of Laplace's equation", *IEEE Transactions on Magnetics*, part II, no.2, vol.33, pp.1216-1218, 1997